

# The 26.3-h orbit and multiwavelength properties of the ‘redback’ millisecond pulsar PSR J1306–40

Manuel Linares<sup>★</sup>

*Departament de Física, EEBE, Universitat Politècnica de Catalunya, c/ Eduard Maristany 10, E-08019 Barcelona, Spain*

Accepted 2017 September 25. Received 2017 September 18; in original form 2017 July 3

## ABSTRACT

We present the discovery of the variable optical and X-ray counterparts to the radio millisecond pulsar (MSP) PSR J1306–40, recently discovered by Keane et al. We find that both the optical and X-ray fluxes are modulated with the same period, which allows us to measure for the first time the orbital period  $P_{\text{orb}} = 1.097\,16[6]$  d. The optical properties are consistent with a main-sequence companion with spectral type G to mid K and, together with the X-ray luminosity ( $8.8 \times 10^{31}$  erg s<sup>-1</sup> in the 0.5–10 keV band, for a distance of 1.2 kpc), confirm the redback classification of this pulsar. Our results establish the binary nature of PSR J1306–40, which has the longest  $P_{\text{orb}}$  among all known compact binary MSPs in the Galactic disc. We briefly discuss these findings in the context of irradiation and intrabinary shock emission in compact binary MSPs.

**Key words:** binaries: general – stars: individual: PSR J1306–40 – stars: neutron – pulsars: general – stars: variables: general – gamma rays: stars.

## 1 INTRODUCTION

New nearby ( $D \lesssim 4$  kpc) millisecond pulsars (MSPs) in compact binaries (orbital periods  $P_{\text{orb}} \lesssim 1$  d) are being discovered in a number of different ways. These include radio timing observations (Hessels et al. 2011; Ray et al. 2012), ‘blind’ pulsation searches (Pletsch et al. 2012) and optical studies (Romani & Shaw 2011; Kong et al. 2012; Salvetti et al. 2015; Linares et al. 2017) of *Fermi*-LAT unidentified GeV sources. Compact binary MSPs are often classified according to the mass of the companion star into ‘black widows’ ( $M_2 \sim 0.01 M_{\odot}$ ) and ‘redbacks’ ( $M_2 \sim 0.1 M_{\odot}$ ; Roberts 2011).

A panchromatic approach to finding new MSPs is important, since the pulsations often prove difficult to detect in the radio and gamma-ray bands, mostly due to occultation and acceleration effects along the orbit, respectively. While systems with  $P_{\text{orb}}$  close to a day have been especially elusive so far, a redback candidate in a 21-h orbit was recently discovered by Linares et al. (2017) and Li et al. (2016). This emergent population of MSPs has potentially far-reaching implications for many fields of astrophysics, ranging from binary evolution (Benvenuto, De Vito & Horvath 2015) and astroparticle physics (Venter et al. 2015) to the maximum neutron star mass and the equation of state at supra-nuclear densities (see e.g. Özel & Freire 2016, and references therein).

The MSP PSR J1306–40 was recently discovered as part of an ongoing radio survey (SUPERB; Keane et al. 2017), with a spin period of 2.2 ms and a dispersion measure indicating a distance of

$D \approx 1.2$  kpc. Even if no orbital solution could be obtained, Keane et al. (2017) suggest that this is a redback-type binary MSP eclipsed during a large fraction of the orbit. In order to confirm or reject this hypothesis, we have studied the multiwavelength properties of PSR J1306–40 from the infrared to the gamma-ray bands. We report our results hereafter, including the discovery of optical and X-ray flux modulations which reveal a 26.3-h orbital period.

## 2 DATA ANALYSIS AND RESULTS

### 2.1 Optical

We searched the Catalina Sky Survey catalogue (CSS; Drake et al. 2009), and found one matching source (SSS J130656.3-403522) at the radio position of PSR J1306–40 (Keane et al. 2017). As we show in Fig. 1 (right), this is the only optical source within the radio error circle. We find a refined optical position from the USNO-B1 catalogue of RA = 13<sup>h</sup>06<sup>m</sup>56<sup>s</sup>.30, Dec. = –40°35′23″.3 (J2000, 0.2 arcsec astrometric uncertainty, Monet et al. 2003; this is 0.6 arcsec from the CSS source position). Thus, our variable optical counterpart’s position is fully consistent with the 7 arcsec-radius radio location. We downloaded the V-band photometric CSS light curve, taken between 2005 and 2012 with the SSS 0.5-m telescope from nightly sequences of typically four 30-s images. In order to reduce the noise in the light curve, we filtered out data taken at airmass > 1.7 or with seeing worse than 7 arcsec, leaving a total of 155 magnitude measurements. We verified that relaxing these filters and using the full data set (with 257 data points) have no impact on the final period reported below. Furthermore, we inspected the

<sup>★</sup> E-mail: manuel.linares@upc.edu

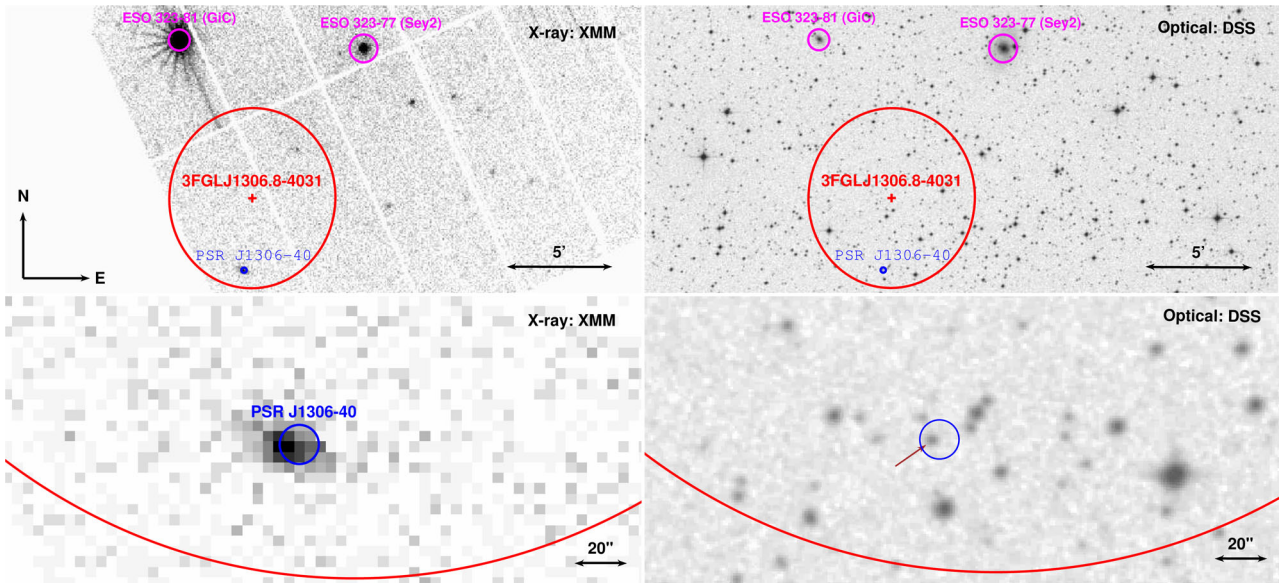


**Figure 1.** Left: an X-ray image of the field of 3FGL J1306.8–4031 (red ellipse) from the longest XMM EPIC-PN observation (top) and zoom into the region of PSR J1306-40 (blue circle; bottom). Two nearby galaxies and bright X-ray sources are marked (magenta circles). Right: an optical DSS image of the field (top) and zoomed finding chart (bottom), showing the radio location of PSR J1306-40 (blue circle) and the variable optical counterpart reported in this work (SSS J130656.3–403522; brown arrow).

CSS light curve rebinned into 50-d bins and found no signs of a state change in the optical band (the long-term averaged  $V$ -band magnitude remains approximately constant).

The CSS light curve shows clear signs of variability, with  $V$  magnitudes generally in the 17.4–18.4 range. We used a Lomb–Scargle periodogram to perform an initial search for periodicities in the 0.1–10 d range, which includes all known redback orbital periods. Despite the aliasing due to nightly sampling and data gaps, we identify the three strongest peaks at 1.10, 1.96 and 2.03 d. Because the X-ray light curve of PSR J1306–40 is modulated with the same  $\sim 1.10$  d period (Section 2.2), which shows the highest power in the Lomb–Scargle periodogram, we focus the rest of our analysis on this. Applying phase dispersion minimization techniques (Stellingwerf 1978), we obtain a refined measurement of the optical photometric period  $P_{\text{opt}} = 1.097\ 16[6]\ \text{d} = 26.3319[14]\ \text{h}$ . We show in Fig. 2 the corresponding optical light curve folded at this period, which reveals one broad maximum and one narrower minimum per cycle. Some of the known redbacks show one maximum per orbital cycle due to the strongly irradiated ‘inner’ face of the companion star (e.g. Breton et al. 2013), while other redbacks feature two maxima per orbit (e.g. Li, Halpern & Thorstensen 2014), due to the change in projected area in the absence of strong irradiation (the so-called ellipsoidal modulation, see Section 3 for further discussion). We closely inspected the Lomb–Scargle periodogram around  $2 \times P_{\text{opt}}$ , and found no periodicities consistent with this value.

## 2.2 X-ray

The X-ray Multi-Mirror Mission (*XMM–Newton*) observed the field of 3FGL J1306.8–4031 on 2006 February 7 (for 29 ks in observation 0300240501) and 2013 January 17 (for 133 ks in observation 0694170101), aiming at a nearby Seyfert 2 galaxy (see Fig. 1, left). This resulted in the serendipitous detection of a fainter X-ray source, 3XMM J130656.2–403523, which matches the radio position of PSR J1306–40 (as pointed out by Keane et al. 2017, see Fig. 1). We analysed the spectrum and light curve of the X-ray counterpart

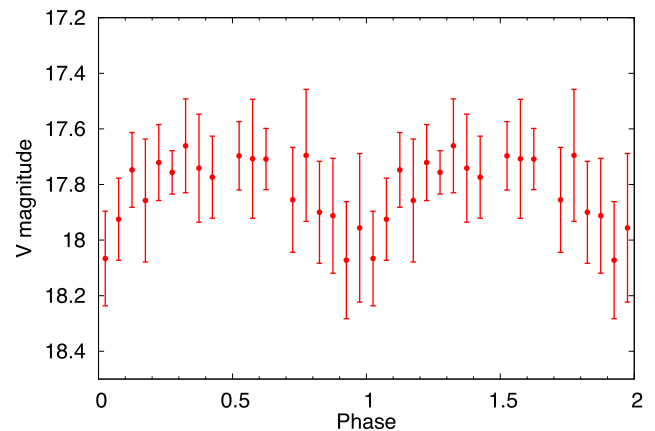


**Figure 2.** The  $V$ -band light curve of the optical counterpart to PSR J1306-40 (SSS J130656.3–403522), folded at the orbital period  $P_{\text{orb}} = 1.097\ 16[6]\ \text{d}$ . The epoch of inferior conjunction of the secondary star ( $T_0 = 56310.421 \pm 0.014\ \text{MJD}$ , which defines phase = 0) is estimated from the X-ray light curve, which is modulated with the same period (see Section 2.2 for details). Two cycles are plotted for clarity.

to PSR J1301-40 from the longest observation, using the pipeline processing system products (*SAS* version 20150701\_1240-14.0.0) and the latest available response matrix (*epn\_e3\_ff20\_sdY5\_v16.0*). The second half of the observation suffered from background flaring periods, which had only minor effects on the background-corrected light curve, but were excluded from the spectral analysis.

The average 0.2–12 keV EPIC-pn spectrum from the 2013 observation is well fitted with an absorbed power-law model (*tbabs\*power* within *XSPEC*; Arnaud 1996) with absorbing column density  $N_{\text{H}} = [6 \pm 1] \times 10^{20}\ \text{cm}^{-2}$ , a photon index  $1.31 \pm 0.04$  and an absorbed 0.5–10 keV flux of  $[4.9 \pm 0.1] \times 10^{-13}\ \text{erg s}^{-1}\ \text{cm}^{-2}$ . The corresponding 0.5–10 keV luminosity for the  $D = 1.2\ \text{kpc}$  distance (Keane et al. 2017) is  $8.8 \times 10^{31}\ \text{erg s}^{-1}$ , fully consistent with that of redback MSPs in the radio pulsar state (which also

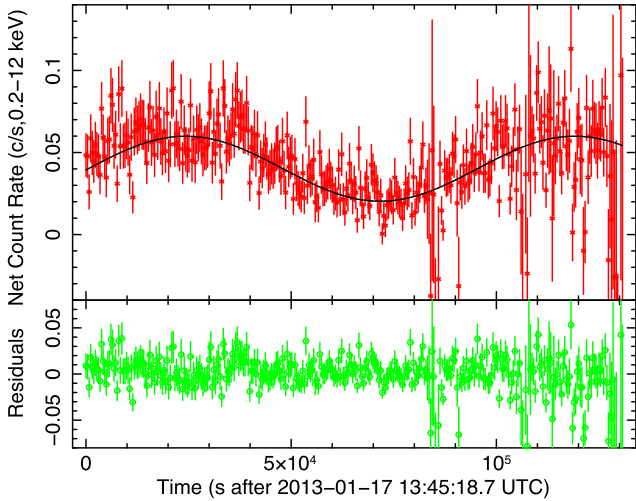


**Figure 3.** XMM light curve of the X-ray counterpart to PSR J1306-40 (top; net 0.2–12 keV count rate), modulated with the same period as the optical light curve. We also show our sinusoidal best-fitting function (black line) and the corresponding residuals (bottom).

feature hard X-ray spectra with photon indices in the 1–2 range; Linares 2014). The 2006 observation shows a similar photon index ( $1.3 \pm 0.1$ ) and a somewhat lower luminosity of  $2.6 \times 10^{31}$  erg s<sup>-1</sup> (i.e. still consistent with the radio pulsar state).

The background-corrected 0.2–12 keV light curve shows a clear nearly sinusoidal modulation (Fig. 3). We fit the light curve with a simple sine model and find that the X-ray ( $P_X$ ) and optical ( $P_{opt}$ ) periods are consistent (within  $2.7\sigma$ ), while the fractional semi-amplitude is large, close to 50 per cent. In particular, a simple sine fit yields  $P_X = 1.14 \pm 0.03$  d and a reduced chi-squared of 1.31 for 342 degrees of freedom. We also show in Fig. 3 the results of fitting the X-ray light curve with a sine function with the period fixed at  $P_{opt}$  (1.097 16 d), which results into a similarly good fit (reduced chi-squared of 1.31 for 343 degrees of freedom).

Interestingly, very similar X-ray orbital modulation is seen in redback and black widow MSPs (Bogdanov et al. 2011; Gentile et al. 2014), with one maximum and one minimum per orbital cycle in the X-ray light curve. Therefore, we conclude that both X-ray and optical light curves of PSR J1306-40 are modulated at the orbital period  $P_{orb} = 1.097\ 16[6]$  d =  $P_{opt} = P_X$ . In those cases, the minimum X-ray and optical fluxes correspond to the same orbital phase (0 in our definition; 0.25 in the radio pulsar definition), when the companion at inferior conjunction is thought to partially occult the X-ray emitting intrabinary shock between the pulsar and the companion winds (Bogdanov et al. 2011). Using this analogy (i.e. assuming that the minimum X-ray flux corresponds to phase = 0) and our best fit to the XMM X-ray light curve, we can constrain the epoch of inferior conjunction of the companion to  $T0 = 56310.421 \pm 0.014$  MJD ( $1\sigma$  statistical uncertainty).

### 3 DISCUSSION

We have presented the discovery of the optical and X-ray counterparts to PSR J1306-40 (Keane et al. 2017), which we show are both modulated with the same period. We thereby find the orbital period of this newly discovered MSP at  $P_{orb} = 1.097\ 16[6]$  d, the longest among the currently known compact binary MSPs in the Galactic disc. The only known redback with a longer  $P_{orb}$  is PSR J1740-5340, in the globular cluster NGC 6397 ( $P_{orb} = 1.35$  d;

D’Amico et al. 2001). The rapid release of sky locations for new candidate or confirmed MSPs allows multiwavelength studies and a more efficient characterization of this growing population.

We note that the orbital X-ray modulation that we have found in PSR J1306-40 (Section 2.2), with an orbital period of about 26.3 h, is very similar to that of the redback PSR J1023+0038, with  $P_{orb} \simeq 4.8$  h. For a  $P_{orb} \sim 5$  times longer (assuming similar total mass), the orbital separation of PSR J1306-40 is  $\sim 3$  times larger. Our results show that in these conditions the shock responsible for the X-ray emission can still be formed and observed. As we discover MSPs with main-sequence companions in wider orbits, we will probe the pulsar wind and its interaction with that of the companion star further away from the pulsar. In particular, comparing shocks at different orbital separations may tell us whether the companion wind is intrinsic/thermal or induced by the pulsar (see e.g. discussion in Harding & Gaisser 1990).

Interestingly, we find one broad maximum and one narrow minimum per orbital cycle in the optical light curve (Section 2.1, Fig. 2). This is different than other redback MSPs with long orbital periods, which tend to show two maxima per cycle (see e.g. Linares et al. 2017, and references therein). Thus, we conclude that irradiation of the companion by the pulsar wind is likely to play an important role in shaping the optical light curve of PSR J1306-40, despite its relatively wide orbit. This might be due to an energetic or beamed MSP wind, to a relatively faint companion or to a combination thereof.

We find no evidence of any optical or X-ray state change between 2005 and 2013, from the available XMM (2006, 2013) and CSS (2005–2012) data sets. Considering also the radio pulsar detections in 2015 June and 2016 September (Keane et al. 2017), and taking into account that accretion disc states may last from months to years, this suggests that PSR J1306-40 has been in the radio pulsar (disc-free) state for at least the last  $\sim 11$  yr.

Our variable X-ray and optical counterparts match a 2MASS source (2MASS J13065627-4035233; Skrutskie et al. 2006) with near-infrared magnitudes of  $J = 16.26 \pm 0.12$ ,  $H = 15.99 \pm 0.17$  and  $K = 15.39 \pm 0.20$ . At longer wavelengths, we find a coincident WISE source (WISE J130656.28-403523.3; Wright et al. 2010), with magnitudes  $w1 = 15.61 \pm 0.04$ ,  $w2 = 15.77 \pm 0.11$ ,  $w3 > 13.0$  and  $w4 > 9.3$ . The NOMAD/USNO-B1 catalogue lists  $B$ ,  $V$ ,  $R$  and  $I$  magnitudes for this object of  $\simeq 18.4$ , 17.7, 18.1 and 17.5, respectively. The reddening from infrared dust maps at the position of PSR J1306-40 (Schlegel, Finkbeiner & Davis 1998) is  $E(B-V) = 0.092 \pm 0.002$  mag, which agrees with the value inferred from our measured  $N_H$  ( $E(B-V) \sim N_H/[3.1 \times 1.8 \times 10^{21} \text{ cm}^{-2}] \sim 0.1$  mag; Predehl & Schmitt 1995). Using this reddening, we estimate an intrinsic colour  $(B-V) \simeq 0.60$ , which is consistent with an early G star (Pecaut & Mamajek 2013).

We find  $V_{CSS} \simeq 18$  mag at minimum (Fig. 2;  $V \simeq 18.15$  mag applying the CSS colour correction<sup>1</sup>), which corresponds to an extinction-corrected  $V \simeq 17.85$ . For the inferred  $D = 1.2$  kpc (Keane et al. 2017), the absolute visual magnitude is  $M_V \sim 7.45$ , close to that of a K5 main-sequence star (Pecaut & Mamajek 2013). Therefore, while more accurate – and phase-resolved optical photometry and spectroscopic measurements are desirable and needed to place tighter constraints on the binary parameters, we can estimate a G-to-mid-K spectral type for the companion to PSR J1306-40. Finally, since all known black widows known are fainter than  $r \sim 19$  mag (e.g. PSR 1957+20, with absolute visual magnitude

<sup>1</sup> <http://nesssi.cacr.caltech.edu/DataRelease/FAQ2.html#improve>

$\simeq 10.5$ ; Djorgovski & Evans 1988), our optical counterpart to PSR J1306-40 strongly favours a redback-type main-sequence companion (unless the distance measured by Keane et al. 2017 from the pulsar's dispersion measure is severely overestimated). The same is true for the X-ray luminosity which we find close to  $10^{32}$  erg s $^{-1}$  (Section 2.2), and which also points to a redback MSP identification.

The *Fermi*-LAT source 3FGL J1306.8–4031 (Acero et al. 2015) includes PSR J1306–40 in its 4.3 arcmin error circle and MSPs are well-known gamma-ray emitters. However, while the flux variability (variability index 44) and 0.1–100 GeV luminosity ( $[2.5 \pm 0.2] \times 10^{33}$  erg s $^{-1}$  at  $D = 1.2$  kpc) are in line with the properties of virtually all LAT-detected MSPs, the GeV spectrum is clearly at odds. 3FGL J1306.8–4031 features a flat spectrum with little or no spectral curvature (curvature significance 0.3), without any apparent cutoff up to at least 10 GeV. This is unlike any LAT spectrum of the known MSPs, with the possible exception of 3FGL J1417.5-4402 (Strader et al. 2015; Camilo et al. 2016): a peculiar binary MSP with a giant companion in a 5.4-d orbit, possibly accreting, which also shows a flat spectrum in the LAT band.

There are no other catalogued LAT sources within at least two degrees of 3FGL J1306.8–4031. However, the field contains two galaxies belonging to the same cluster, only 8.8 arcmin and 8.3 arcmin from the centre of the LAT position: ESO 323-77 (classified as Seyfert 2) and ESO 323-81, respectively. Both galaxies are bright X-ray sources (see Fig. 1, top left panel), and active galaxies are known GeV emitters. Since *Fermi*-LAT has an angular resolution of about 9 arcmin or worse, we suggest that the LAT source is actually a blend of PSR J1306-40 and the nearby galaxies in the field. That would attribute the flat spectrum to contamination from the nearby galaxies, and it would also explain why 3FGL J1306.8–4031 is not centred around PSR J1306-40 but rather shifted towards the two galaxies (Fig. 1, top). Detailed reanalysis of this LAT field may be able to address this issue and resolve multiple sources. That would in turn yield a more reliable measurement of the MSP gamma-ray flux, and perhaps its orbital or spin modulations.

## ACKNOWLEDGEMENTS

In memory of our esteemed colleagues Enrique García-Berro and Àngels Riera. We thank A. Harding for a discussion on MSP gamma-ray spectra, and specifically for pointing out the possibility of source confusion in the *Fermi*-LAT band, and J. Strader for pointing out the case of 3FGL J1417.5-4402. We thank G. Sala and A. Drake for guidance and suggestions on XMM and CSS data products, respectively, P. Rodríguez-Gil for useful comments on an early draft and the anonymous referee for a thorough review which improved this manuscript. This publication has made use of the SIMBAD data base, operated at CDS-Strasbourg-France, data obtained from the 3XMM *XMM-Newton* serendipitous source catalogue compiled by the 10 institutes of the XMM-Newton Survey Science Centre, as well as data products provided by HEASARC, 2MASS and *WISE*. The CSS survey is funded by the National Aeronautics and Space

Administration under grant no. NNG05GF22G issued through the Science Mission Directorate Near-Earth Objects Observations Program. CRTS and CSDR2 are supported by the U.S. National Science Foundation under grant Ast-1413600. Based on photographic data obtained using The UK Schmidt Telescope. The Digitized Sky Survey was produced at the Space Telescope Science Institute under US Government grant NAG W-2166. ML is supported by EU's Horizon 2020 programme through a Marie Skłodowska-Curie Fellowship (grant no. 702638).

## REFERENCES

- Acero F. et al., 2015, *ApJS*, 218, 23  
 Arnaud K. A., 1996, in Jacoby G. H., Barnes J., eds, *ASP Conf. Ser. Vol. 101, Astronomical Data Analysis Software and Systems V*. Astron. Soc. Pac., San Francisco, p. 17  
 Benvenuto O. G., De Vito M. A., Horvath J. E., 2015, *MNRAS*, 449, 4184  
 Bogdanov S. et al., 2011, *ApJ*, 730, 81  
 Breton R. P. et al., 2013, *ApJ*, 769, 108  
 Camilo F. et al., 2016, *ApJ*, 820, 6  
 D'Amico N., Possenti A., Manchester R. N., Sarkissian J., Lyne A. G., Camilo F., 2001, *ApJ*, 561, L89  
 Djorgovski S., Evans C. R., 1988, *ApJ*, 335, L61  
 Drake A. J. et al., 2009, *ApJ*, 696, 870  
 Gentile P. A. et al., 2014, *ApJ*, 783, 69  
 Harding A. K., Gaisser T. K., 1990, *ApJ*, 358, 561  
 Hessels J. W. T. et al., 2011, in Burgay M., D'Amico N., Esposito P., Pellizzoni A., Possenti A., eds, *AIP Conf. Ser. Vol. 1357*. p. 40  
 Keane E. F. et al., 2017, *MNRAS*, preprint ([arXiv:1706.04459](https://arxiv.org/abs/1706.04459))  
 Kong A. K. H. et al., 2012, *ApJ*, 747, L3  
 Li M., Halpern J. P., Thorstensen J. R., 2014, *ApJ*, 795, 115  
 Li K.-L., Kong A. K. H., Hou X., Mao J., Strader J., Chomiuk L., Tremou E., 2016, *ApJ*, 833, 143  
 Linares M., 2014, *ApJ*, 795, 72  
 Linares M., Miles-Pérez P., Rodríguez-Gil P., Shahbaz T., Casares J., Fariña C., Karjalainen R., 2017, *MNRAS*, 465, 4602  
 Monet D. G. et al., 2003, *AJ*, 125, 984  
 Özel F., Freire P., 2016, *ARA&A*, 54, 401  
 Pecaat M. J., Mamajek E. E., 2013, *ApJS*, 208, 9  
 Pletsch H. J. et al., 2012, *Science*, 338, 1314  
 Predehl P., Schmitt J. H. M. M., 1995, *A&A*, 293  
 Ray P. S. et al., 2012, preprint ([arXiv:1205.3089](https://arxiv.org/abs/1205.3089))  
 Roberts M. S. E., 2011, in Burgay M., D'Amico N., Esposito P., Pellizzoni A., Possenti A., eds, *AIP Conf. Ser. Vol. 1357*. p. 127  
 Romani R. W., Shaw M. S., 2011, *ApJ*, 743, L26  
 Salvetti D. et al., 2015, *ApJ*, 814, 88  
 Schlegel D. J., Finkbeiner D. P., Davis M., 1998, *ApJ*, 500, 525  
 Skrutskie M. F. et al., 2006, *AJ*, 131, 1163  
 Stellingwerf R. F., 1978, *ApJ*, 224, 953  
 Strader J. et al., 2015, *ApJ*, 804, L12  
 Venter C., Kopp A., Harding A. K., Gonthier P. L., Büsching I., 2015, *ApJ*, 807, 130  
 Wright E. L. et al., 2010, *AJ*, 140, 1868

This paper has been typeset from a  $\text{\TeX}/\text{\LaTeX}$  file prepared by the author.